

Evidence for charged defects in intrinsic glow-discharge hydrogenated amorphous-silicon-germanium alloys

Chih-Chiang Chen, Fan Zhong,* and J. David Cohen

Department of Physics, University of Oregon, Eugene, Oregon 97403

Jeffrey C. Yang and Subhendu Guha

United Solar Systems Corporation, 1100 West Maple Road, Troy, Michigan 48084

(Received 22 December 1997)

We have applied drive-level capacitance profiling, transient photocapacitance, and junction transient photocurrent measurements to characterize the defect-state distribution for a set of device-quality glow-discharge *a*-Si,Ge:H films. The combination of the latter two methods can distinguish majority- from minority-carrier optical transitions. Comparing the optical spectra of intrinsic samples with those in *p*-type and *n*-type samples, we have concluded that significant densities of positively and negatively charged deep defects exist in intrinsic glow-discharge *a*-Si,Ge:H alloys. Our measurements also indicate how the density of these charged defects increase upon light-induced degradation and how they affect carrier recombination processes.

[S0163-1829(98)52208-4]

Amorphous-silicon-germanium alloys (*a*-Si,Ge:H) have attracted considerable interest recently because of their importance in thin-film tandem and triple photovoltaic cells. To understand the electronic properties of these alloys, a key ingredient is the detailed structure of their deep defects and how these affect carrier dynamics. Defect level evaluation methods such as the constant photocurrent method (CPM) or photothermal deflection spectroscopy¹⁻⁶ have not been found to be good predictors of *a*-Si,Ge:H photovoltaic device performance.⁶ Indeed, a serious shortcoming of such methods is that they cannot distinguish the *type* of optical transition; i.e., those that remove an electron from a filled defect level to the conduction band and those that insert valence-band electrons into empty defect levels. This ambiguity precludes identifying the defect levels involved and, therefore, the specific consequences of these defect states on the majority- and minority-carrier processes.

In this paper we report a detailed evaluation of the thermally and optically induced defect transitions in a series of device-quality glow-discharge *a*-Si,Ge:H samples using junction capacitance and photocurrent methods. The combination of the junction photocapacitance and photocurrent spectroscopies can clearly identify the *type* of defect transition. Comparing such spectra in both intrinsic and lightly *p*- and *n*-type doped samples firmly establishes that charged defects exist in significant concentrations in intrinsic *a*-Si,Ge:H alloys.

For this study, nine *a*-Si,Ge:H alloy samples were deposited by the rf glow-discharge method onto heavily *p*⁺-doped crystalline silicon substrates at United Solar Systems Corporation.⁷ Properties of the samples are listed in Table I. Seven had Ge fractions in the technologically important 30–35 at. % range; however, a 20 and a 50 at. % Ge sample were also included. Five samples were very close to intrinsic, one was *n*-type doped with 2 Vppm PH₃ during growth, one was *p*-type doped with 6 Vppm BF₃, and two others were unintentionally doped with trace levels of PH₃. These last

two samples, with 50–100 meV shallower Fermi levels than the most intrinsic samples, will be referred to as “*ν* type.” For studies of the intrinsic, the *n*- and *ν*-type doped samples we evaporated semitransparent Pd top contacts onto each but

TABLE I. Properties of *a*-Si,Ge:H films studied, including Fermi-level positions deduced by ac admittance, the TH1 defect density deduced by drive-level capacitance profiling, and the defect bands of optical transition, OP1 and OP2, deduced from the transient photocapacitance plus photocurrent spectra. The error bars for TH1 reflect the spatial variations of the profiles obtained. The absolute densities for OP1 and OP2 depend on assumed optical cross sections that are unknown to within a factor of 10; however, relative errors, as determined from the fitting statistics, are only $\pm 4\%$ and $\pm 8\%$ for OP1 and OP2, respectively.

Ge at. % (doping)	State	$E_c - E_f$ (eV)	TH1 ($10^{15}/\text{cm}^3$)	OP1 ($10^{16}/\text{cm}^3$)	OP2 ($10^{16}/\text{cm}^3$)
20 at. % (intrinsic)	A	0.73	2.4 ± 0.3	0.64	1.88
	B	0.75	6.5 ± 0.6	1.46	3.62
30 at. % (intrinsic)	A	0.70	6.0 ± 0.3	1.99	5.18
	B	0.75	13.7 ± 0.9	6.63	7.54
35 at. % (intrinsic)	A	0.71	6.3 ± 0.4	4.38	4.42
	B	0.73	14.0 ± 1.2	7.91	7.73
35 at. % (intrinsic)	A	0.75	6.0 ± 0.3	2.56	4.82
	B	0.75	14.5 ± 1.2	7.32	8.93
50 at. % (intrinsic)	A	0.67	63.0 ± 3.0	29.5	51.3
	B	0.64	90.0 ± 5.0	31.6	49.2
35 at. % (<i>ν</i> type)	A	0.66	8.0 ± 0.4	3.86	1.34
	B	0.75	18.6 ± 0.9	4.15	3.93
35 at. % (<i>ν</i> type)	A	0.65	10.7 ± 0.1	2.29	1.25
	B	0.69	20.4 ± 1.3	4.07	4.05
35 at. % (<i>n</i> type)	A	0.56	60.0 ± 2.5	43.8	0.00
	B	0.64	90.2 ± 6.0	69.9	0.00
35 at. % (<i>p</i> type)	A	>0.80		0.0	21.0

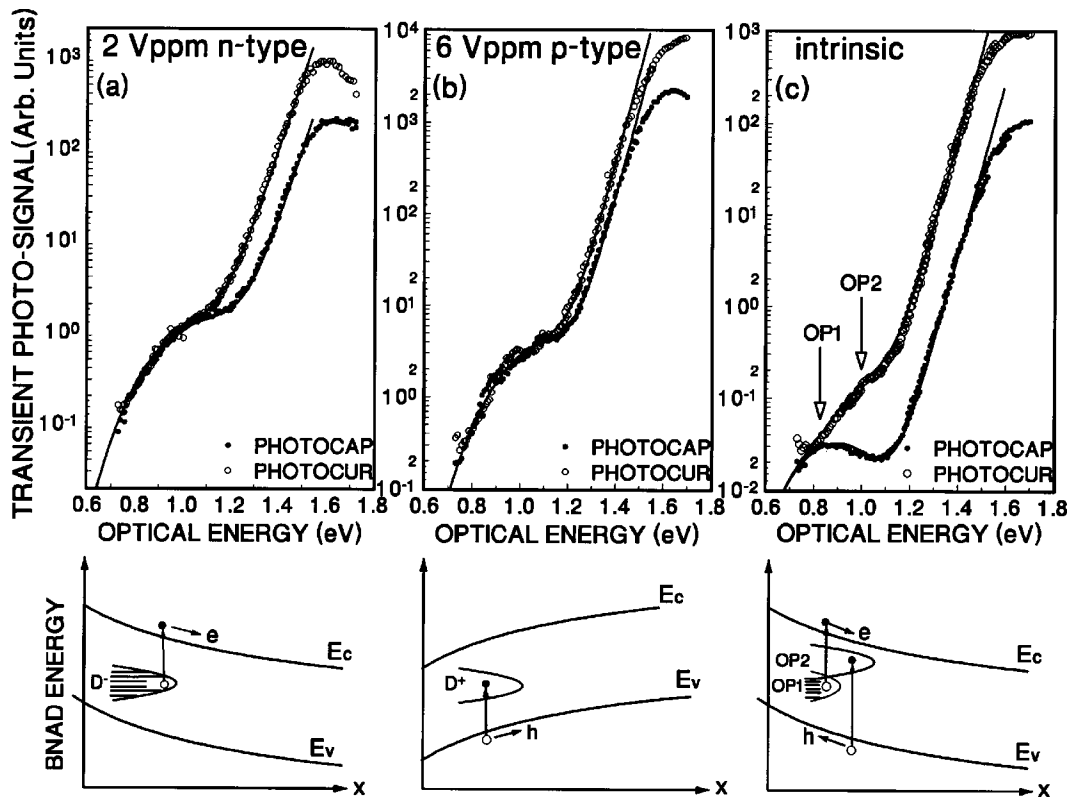


FIG. 1. Pairs of photocapacitance and photocurrent spectra for three 35 at. % *a*-Si,Ge:H samples: (a) *n*-type doped, (b) *p*-type doped, and (c) intrinsic. The thin lines through the data points are fits using the types of defect optical transitions indicated below each set of spectra (together with an exponential distribution of band tail states).

employed the junction at the p^+ *c*-Si substrate for our measurements. For the *p*-type sample we grew a thin n^+ *a*-Si:H layer on top of the film and used the resulting n^+p heterojunction for our measurements.

All samples were annealed at 460 K for 1 h before the initial series of measurements (state A). To study the degraded state, samples were light soaked with an appropriate long pass filter to achieve uniform carrier generation rates. Light exposure on *a*-Si,Ge:H alloys was at 6 W/cm² for 70 h with the samples immersed in methanol to maintain a surface temperature below 65 °C (state B). Four types of measurements were performed on each sample: (1) Admittance vs temperature at a series of fixed frequencies (10 Hz, 100 Hz, 1 kHz, and 10 kHz) to establish the activation energies of conductivity E_σ ; (2) drive-level capacitance profiling (DLCP) at 10 or 100 Hz at a series of temperatures to quantitatively determine the charge density in the deep depletion region of each sample junction.⁸ For the *n*-type and intrinsic samples, this charge density indicates the deep defects that can lose an electron via thermal excitation to the conduction band. Finally, we recorded (3) transient photocapacitance (TPC) and (4) transient junction photocurrent (TPI) spectra for each sample at several temperatures in both the annealed and light soaked states. As has been previously described in some detail,^{9,10} the TPC method records the residual charge change due to weak optical excitation within the depletion region on the measurement time scale (400 ms in our case). Because transitions to the majority band increase the depletion capacitance, while transitions to the minority band decrease the depletion capacitance, the TPC spectra indicate the *difference* between these two types of transitions. On the

other hand, the current due either to majority or to minority carriers has the same sign; therefore, the TPI spectra reveal the *sum* of the two types of transitions. Taken together, these two types of spectra allow one to identify whether defect transitions involve the majority- or minority-carrier bands. Also, it is generally accepted that *a*-Si,Ge:H alloys with Ge fractions larger than about 25 at. % contain virtually no Si dangling bonds.^{11,12} Thus we will assume that all deep defect transitions originate from the different charge states of Ge dangling-bond (*D*) defects.

Figure 1(a) shows TPC and TPI spectra (measured at 350 K) for the 2 Vppm *n*-type doped sample. A dc potential of 3 V was applied to place the substrate p^+n junction into reverse bias. Here the spectra are fit using only a single defect subband with electronic excitations to the conduction band. This subband should correspond to D^- centers because these dominate at even moderate *n*-type doping levels. Because only an electron current results from the optical transitions of this defect subband, both the TPI and TPC spectra are seen to overlap perfectly outside of the band tail regime. On the other hand, within the band tail region, each optical transition results in one conduction-band electron plus one valence-band hole. This leads to a distinct decrease in the TPC relative to the TPI spectrum due to the motion of the hole. The magnitude of this decrease actually depends on the relative carrier mobilities and has been used to estimate the hole $\mu\tau$ product in several previous studies.¹³⁻¹⁶

Figure 1(b) shows the optical spectra obtained at 350 K for the 6 Vppm *p*-type doped sample. Here we also find only a single defect subband of optical transitions is needed to fit the spectra. This now corresponds to D^+ defects. This

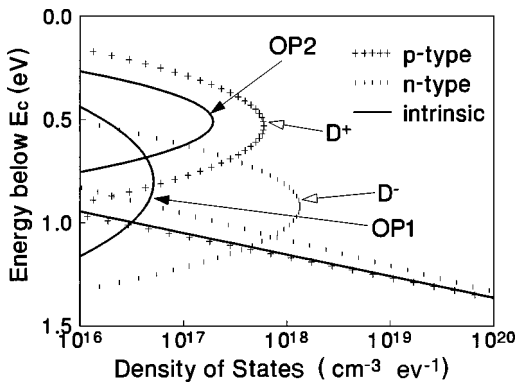


FIG. 2. Energy distributions of defect bands used to fit the three sample spectra of Fig. 1. Note the good match between the D^+ band of the p -type sample and the OP2 band of the intrinsic sample.

sample incorporates a thin n^+ a -Si:H on top of the film and the band bending in the major depletion region (again under 3 V bias) is at the top junction and is *downward*.¹⁷ Therefore, it is now the majority *hole current* induced by the optical transition that is responsible for the TPI and TPC signals (this is confirmed by the *sign* of the TPC signal). The perfect overlap of these two spectra outside the band tail region verifies that there is only a single type of defect transition involved.

Figure 1(c) shows a typical spectra for a 35 at. % Ge intrinsic sample. Here things have obviously become more complex. Indeed, we now need *two* bands of defect transitions to fit the spectra. One corresponds to optical transitions that remove an electron from a defect subband into the conduction band, while the other corresponds to transitions that insert a valence-band electron into an unoccupied defect subband. We have previously denoted these two bands of optical transitions as “OP1” and “OP2,” respectively.^{15,18} Like the case for the n -type film, the major depletion region for the intrinsic samples is at the substrate junction with an upward band bending. Also, because the Fermi level is slightly closer to the conduction band, the optically induced current *at threshold* will be totally due to electrons excited out of defect levels. Therefore, the TPC and TPI spectra should be strictly proportional at these lowest optical energies and so we overlap them in this region. While the optical transitions for the OP1 subband will continue to contribute equally to the TPC and TPI spectra, the hole current arising from OP2 subband of optical transitions will contribute oppositely to the TPC and TPI signals. This results in the large separation of the two spectra at intermediate optical energies.

The intrinsic sample spectra actually exhibit a separation that is larger near 1.1 eV than in the band tail region (above 1.3 eV). As we have discussed previously,^{10,15,18} this implies that the valence-band electrons inserted into the OP2 defect subband are not released for times longer than the measurement time window (0.4 s). Thus we had hypothesized that the responsible defect subband for OP2 would more likely correspond to D^+ (rather than D^0) Ge dangling bonds since these would have a large thermal barrier for reemission of the electrons being optically inserted from the valence band.

The optical defect transition bands for the three samples of Fig. 1 are summarized in Fig. 2. We can see clearly that the OP2 subband is nearly identical in energy to the D^+

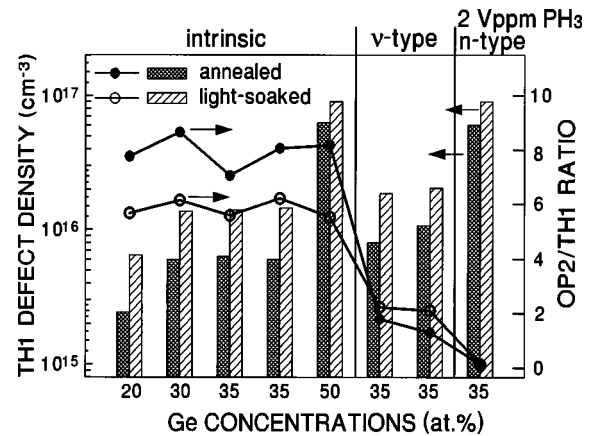


FIG. 3. Bar graphs indicating magnitudes of the DLCP determined TH1 band in the annealed and light soaked states (left-hand logarithmic scale) along with the OP2/TH1 ratios in each case (right-hand linear scale). The nearly constant ratio for the intrinsic samples, and the decreasing ratio for the ν - and n -type samples, strongly suggest that TH1 is associated with the D^- subband.

defect subband in the p -type sample and this confirms its identification with this subband. Therefore, these optical spectra clearly demonstrate that there are significant positively charged defects in intrinsic glow-discharge a -Si,Ge:H alloys. Because of charge neutrality, there must also exist similar density of negatively charged defect states in these samples. However, the OP1 subband of the intrinsic samples has a different shape and energy position compared to the D^- defect subband in the n -type sample. Therefore, the OP1 subband is probably *not* a reliable indicator of the magnitude of the D^- defect subband (that is, it more likely involves transitions from a *superposition* of the D^- and D^0 subbands).

Instead, consider the DLCP method. This depends on the thermal emission of trapped charge to the majority-carrier band so that the detected transitions (denoted as “TH1”) in intrinsic and n -type samples correspond to deep defects containing at least one electron. Moreover, because electrons bound to D^- defects are more easily thermally emitted, TH1 is more likely to be a good indicator of the D^- defect density. Indeed, Fig. 3 shows that, for the 35 at. % Ge samples, the TH1 density increases as the n -type doping level increases. From Table I we also see that the OP2 density determined by the TPC and TPI methods exhibits a decreasing trend with increasing n -type doping, again consistent with our identification of OP2 with the D^+ defect subband.

In Fig. 3 we have also plotted the *ratio* of OP2/TH1 for all the samples and see that it is nearly identical for all intrinsic samples in the annealed state and also in the light soaked states. This correlation between the TH1 and the OP2 defect subbands strongly suggests that the TH1 defect subband indeed corresponds to D^- centers by charge neutrality. Also, we see that the OP2/TH1 ratios become smaller for the ν -type samples as would be expected for the D^+/D^- ratios. Finally, the D^+/D^- ratios should increase in the ν -type samples after light soaking and this is also indicated. All of these results strengthen our argument that TH1 defect subband corresponds to D^- centers while OP2 corresponds to D^+ centers. Also, since the DLCP measurements provide an absolute value for the defect density while the optical mea-

surements depend on estimates of optical cross sections, this identification provides a better calibration of the actual defect densities in these samples. That is, the densities listed for OP2 should probably be divided by roughly a factor of 6–8 to match the values of TH1 in the most intrinsic samples.

We have previously made estimates of the values of the mobility lifetime product for holes $(\mu\tau)_h$ for these alloy samples and found that these are nearly inversely proportional to the TH1 densities (to within a factor of 2) independent of metastable state, doping level, or Ge concentration.¹⁶ This is consistent with the idea that recombination is dominated by the initial capture of holes into D^- states. However, there seem to be additional factors that determine carrier lifetimes in the most intrinsic samples. This might imply that carrier capture into neutral defects cannot be ignored. Indeed, because our methods do not provide a clear signature for the density of neutral defects, we do not yet have a good estimate for the ratio of charged to neutral defects. Experiments to compare electron spin resonance (ESR) measurements

with the results of the above types of studies are planned for the near future to pin down this ratio.

Finally, we note that when these types of measurement methods were previously applied to amorphous-silicon samples (a -Si:H), they did *not* yield any such evidence for charged defects.^{9,13} Moreover, comparison studies between ESR and capacitance studies in a -Si:H have indicated fairly consistent agreement between densities of deep defects.¹⁹ This tends to suggest a predominance of *neutral* defects in intrinsic a -Si:H. Thus there appears to be a fundamental difference between a -Si:H and the a -Si,Ge:H alloys. This may be due to the lower correlation energy for Ge vs Si dangling bonds, or to larger potential fluctuations in the alloys. In any case, the recognition of large densities of charged defects in the alloys must significantly alter any future analyses of a -Si,Ge:H based photovoltaic devices.

This work was supported by NREL under Subcontract No. XAN-4-13318-07 at the University of Oregon and under Subcontract No. ZAN-4-13318-02 at United Solar System Corporation.

*Present address: dpix—A Xerox Company, 3406 Hillview Ave., Palo Alto, CA 94304.

¹S. Aljishi, Z. E. Smith, and S. Wagner, in *Amorphous Silicon and Related Materials*, edited by H. Fritzsche (World Scientific, Singapore, 1989), pp. 887–938.

²P. Della Sula, C. Reita, G. Conte, F. Galluzzi, and G. Grillo, *J. Appl. Phys.* **67**, 814 (1990).

³D. Comedi and I. Chambouleyron, *Appl. Phys. Lett.* **53**, 12 566 (1996).

⁴B. Ebersberger, W. Kruhler, W. Fuhs, and H. Mell, *Appl. Phys. Lett.* **65**, 1683 (1994).

⁵Akihisa Matsuda and Gautam Ganguly, *Appl. Phys. Lett.* **67**, 1274 (1995).

⁶X. Xu, J. Yang, and S. Guha, *Appl. Phys. Lett.* **62**, 1399 (1993).

⁷S. Guha, J. S. Payson, S. C. Agarwal, and S. R. Ovshinsky, *J. Non-Cryst. Solids* **97&98**, 1455 (1987).

⁸C. E. Michelson, A. V. Gelatos, and J. D. Cohen, *Appl. Phys. Lett.* **47**, 412 (1985).

⁹J. D. Cohen and A. V. Gelatos, in *Amorphous Silicon and Related Materials* (Ref. 1), pp. 475–512.

¹⁰J. D. Cohen, T. Unold, and A. V. Gelatos, *J. Non-Cryst. Solids* **141**, 142 (1992).

¹¹M. Stutzmann, R. A. Street, C. C. Tsai, J. B. Boyce, and S. E. Ready, *J. Appl. Phys.* **66**, 569 (1989).

¹²The lack of any Si dangling-bond signal in light-induced ESR

measurements of a -Si,Ge:H argues against the possibility even of *charged* Si dangling bonds. See, for example, J. Hautala and J. D. Cohen, in *Amorphous Silicon Technology—1993*, edited by E. A. Schiff *et al.*, MRS Symposia Proceedings No. 297 (Materials Research Society, Pittsburgh, 1993), p. 667.

¹³A. V. Gelatos, K. K. Mahavadi, and J. D. Cohen, *Appl. Phys. Lett.* **53**, 403 (1988).

¹⁴T. Unold, J. D. Cohen, and C. M. Fortmann, *J. Non-Cryst. Solids* **137&138**, 809 (1991).

¹⁵C. C. Chen, F. Zhong, and J. D. Cohen, in *Amorphous Silicon Technology—1996*, edited by M. Hack *et al.*, MRS Symposia Proceedings No. 420 (Materials Research Society, Pittsburgh, 1996), p. 581.

¹⁶C. C. Chen, F. Zhong, J. D. Cohen, J. C. Yang, and S. Guha, in *Amorphous and Microcrystalline Silicon Technology—1997*, edited by S. Wagner *et al.*, MRS Symposia Proceedings No. 467 (MRS, Pittsburgh, 1997), p. 55.

¹⁷This is confirmed by measuring the sign of the photocurrent for short wavelength light.

¹⁸F. Zhong, J. D. Cohen, J. C. Yang, and S. Guha, in *Amorphous Silicon Technology—1994*, edited by E. A. Schiff *et al.*, MRS Symposia Proceedings No. 336 (Materials Research Society, Pittsburgh, 1994), p. 493.

¹⁹T. Unold, J. Hautala, and J. D. Cohen, *Phys. Rev. B* **50**, 16 985 (1994).